HEFAT2014
10th International Conference on Heat Transfer, Fluid Mechanics and Thermodynamics
14 – 26 July 2014
Orlando, Florida

A COMPUTATIONAL STUDY OF CARGO VAN AERODYNAMICS

Abdel-Salam T.* and Chen D.
*Author for correspondence
Department of Engineering,
East Carolina University,
Greenville, NC 27858,
USA,
E-mail: abdelsalamt@ecu.edu

ABSTRACT

In the modern era, various forms of transportation are made and put to use every day. Comparing the vehicles nowadays to the time when the first car was invented, the vehicles nowadays are expected to endure all sorts of abuses, whether it is from the environment or from accidents. Innovative ideas, better visualization, reduced time in the design process, and cost effective "computational testing" is all put together is the use of Computational Fluid Dynamics. The present study numerically investigates the flowfield around a cargo van model. A three-dimensional model of the van is used. Numerical results are obtained using a finite volume CFD code with unstructured grids with size of about 500,000 cells. The governing equations for this study are Navier-Stokes equations. The turbulence model used is the k-ε model. Different free stream velocities ranging from about 43 km/hr to 140 km/hr have been examined. Effects of free stream velocity on the wake region and on the velocity flowfield results are presented. Results show ta significant wake region behind the model. It is noted that the free stream velocity plays slight role in the location of the wake region behind the van.

INTRODUCTION

The importance of aerodynamics is recognized in many fields such as aircraft industry, space flight, missiles, wind engineering, automobiles, and the automobile racing arena. A thorough analysis of aerodynamic properties will aid in the reduction of fuel consumption and also improve the driving characteristics of the vehicle [1]. In this paper we restrict our attention to the study of aerodynamics and its importance in the automobile industry. In today's engineering world, Computational Fluid Dynamics (CFD) codes are used in aiding the prediction of the aerodynamic flow around grounded vehicles [2-9]. Computational Fluid Dynamics (CFD) can be of paramount importance in the analysis of complex fluid flow fields. The external aerodynamic flow field for car and truck geometries is extremely complex. Wind tunnel testing for the car can be very costly and in general only supply the gross characteristics of the flow field such as total drag force. Computational fluid dynamics has the capability of providing much more refined details of the flow field which can be used to optimize the car aerodynamic performance at a reduced fuel consumption level. This can markedly increases the car efficiency and stability, particularly at high speeds. Several studies have been made regarding the alteration of the shape of the vehicle. In Lienhart and Becker's research [10], measurements were performed around an Ahmed model for two different rear slant angles: 25 degrees and 35 degrees. The results show that the two slant angles bracket a critical instability when the flow detaches from the slanted surface [10]. Krajnovic and Davidson [11] used a method called the Large-Eddy simulation to test a simplified car model. The experiment involved testing the flow at different levels of Reynolds number. When the Reynolds number is high, the flow becomes insensitive to the Reynolds number. Their results indicated that instead of the viscosity, the geometry of the vehicle is what dictates the character of the flow and the position of the flow separation. There assumptions states that flow around real cars can be simulated with Large-Eddy Simulation at reduced Reynolds number [11].

To optimize vehicle performance, the forces of air on the body must be accurately obtained and to gain stability through increased down force and reduced side loads while reducing drag is of paramount importance. The engine power consumed by drag increases with the cube of the velocity and therefore at speeds found in the racing community, it must be minimized. Similarly if the automobile has a low down force it can lose control in turns that may result in an accident and driver injury. Hence, optimizing the automobile body shape which will reduce the drag and increase the down force will at the same time increase control and stability and improving performance and fuel economy. In 1984, Ahmed and Ramm [12] performed an extensive set of experiments for a three dimensional body that represented an automobile bluff body separation. The results gave an understanding of the flow pattern around bluff bodies and the ensuing wake behind them. By varying the angle

of the rear body section, the dependence of the body shape on the wake structures and the drag was investigated. With the basic shape and dimensions of the body constant but the back angle of the body was varied 0-30 degrees with respect to the horizontal in five degree increments. The flow structures were measured using a laser velocimeter and the drag generated was also measured. The details of the flow structures and the changes in drag due to the change in the back angle were measured and can provide a good experimental database for validation of CFD studies. It was found that the main contributing factor to the drag force was due to the separation region and the vortices, which formed behind the body. The magnitude of the drag coefficient is directly related to the size and strength of the vortices formed behind the body. The experimental data by Ahmed were utilized in many studies [13-15]. Viswanath [13] conducted a brief study on the pattern of separated flows and its effect on the drag of the body and the wake. In this study different bluff body shapes were chosen to get an understanding of the phenomenon of bluff body flow separation. In this experiment multi-step after-bodies were used to investigate the effects of flow separation on the drag. The experiments showed that the separated flow region was directly related to the length and height of the step. From the drag measurements on the body, it was concluded that the overall drag reduction was not as good as in Ahmed's experiments and suggested the importance of back slant angle on the drag of the body. In the present study the analysis of the flow structure around a passenger van is studied. A Ford passenger van is modeled and simulated at different speeds.

NOMENCLATURE

k	[m^2/s^2]	Turbulent kinetic energy
p	[N/m^2]	Pressure
u	[m/s]	Axial velocity
U	[m/s]	Free stream velocity
x	[m]	Streamwise coordinate
y	[m]	Lateral coordinate
z	[m]	Vertical coordinate

Special characters

δ_{ij}	[-]	Kronecker delta
ε	[m^2/s^2]	Dissipation rate
μ	[N s/m^2]	Dynamic viscosity
ν	[m^2/s]	kinematic viscosity
ρ	[kg/m^3]	Density
s_k	[-]	Turbulent Prandtl number
τ_{ij}	[m/s]	Specific Reynolds-stresses tensor

PHYSICAL MODEL

The physical model in the present study is a cargo van similar to the Ford commercial cargo vans. The length of the van has the following dimensions: length of about 540 cm, body width of about 200 cm and a body height of about 212 cm. The model was created in the commercial CAD program Solid Works then exported to ANSYS Gambit for grid generation. The model is shown in Figure 1.

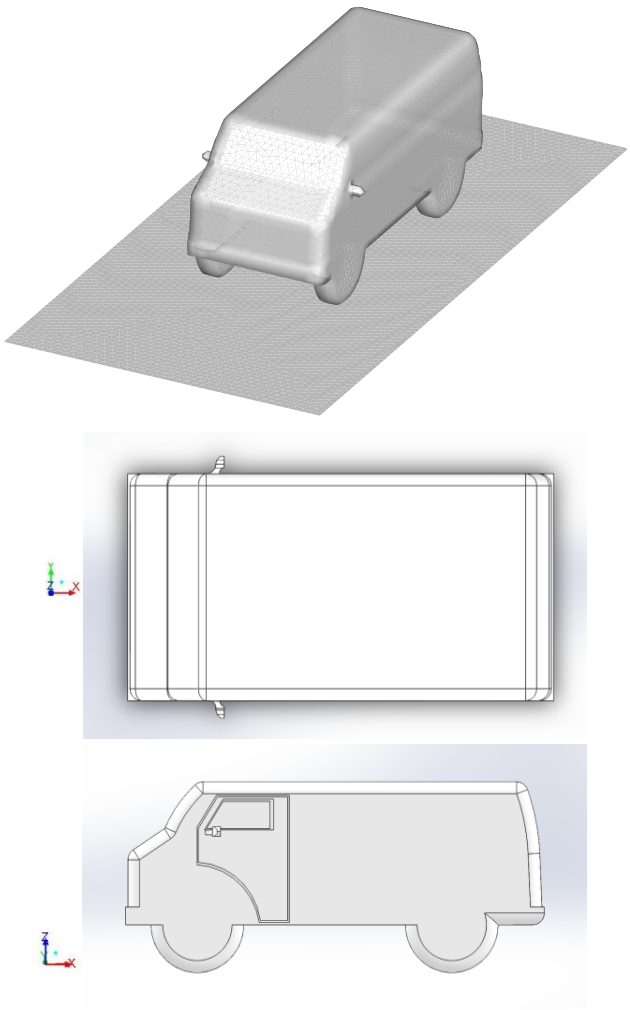

Figure 1 The physical model of the current study (cargo van).

NUMERICAL DETAILS

Governing equations

In the present study the numerical analysis was carried out using a finite volume code for solving the Reynolds-averaged Navier-Stokes equations (ANSYS Fluent [16] and Gambit is the grid generator for Fluent). The important task in Gambit is to get a "good" mesh that captures important flow gradients. This is imperative to achieve accurate results. In order to get accurate results and to save the computational time the mesh should be fine in regions of large flow gradients. For this problem a fine mesh was used in the viscous layers close to the body of the van and in the body wake to accurately model the complex flow in that region. The model is meshed by first meshing the edges of the domain. Meshing of the edges is done to have better control of mesh on the domain so that one can have a fine grid near the surface and coarse grid away from the

body. A multi-block unstructured grid was constructed. Once the meshing is complete assigning the boundary conditions in Gambit so as to specify the conditions at the external boundaries such as wall, inlet etc. is done. A grid of about 500,000 is used in all cases. The boundary conditions are specified at the boundaries and the continuum properties that define a physical characteristic of the model defined by a set of boundary conditions are to be mentioned. Once the boundary conditions are defined and the continuum properties are assigned the mesh is exported so that it can be read into ANSYS Fluent. Reynolds averaging was used to time average the instantaneous full Navier-Stokes equations to produce Reynolds-averaged equations of fluid motion which are better suited to predict the velocity field of a turbulent flow. Assuming the flow is steady and gravity is negligible, the incompressible form of the continuity and the momentum equations in Cartesian tensor notation are

$$\frac{\partial U_i}{\partial x_i} = 0 \tag{1}$$

$$\rho_{U\,j} \frac{\partial U_i}{\partial x_j} + \frac{\partial P}{\partial x_i} - \frac{\partial \tau_{ij}}{\partial x_j} = 0 \tag{2}$$

where x_i represents the Cartesian coordinates, U_i represent the Cartesian time-averaged velocity components, p represents the time-averaged pressure, and τ_{ij} is the stress tensor given by

$$\tau_{ij} = \left[\mu \left(\frac{\partial U_i}{\partial x_j} + \frac{\partial U_j}{\partial x_i} \right) \right] - \frac{2}{3} \mu \frac{\partial U_i}{\partial x_i} \delta_{ij} \tag{3}$$

Turbulence model

A variety of turbulence models that can be used based on the problem being solved. The four turbulence models are the standard k-ε turbulence model, the Large Eddy simulation (LES) model, a Reynolds stress model (RSM), and the Spalart Allmaras model. The Spalart Allmaras model takes the least computational effort and a one-equation algebraic model. This model works well when the flow remains attached over the body. The k-ε model solves two differential equations and the computational effort is increased however it works well for flows with small regions of flow separation. The RSM model has the capability to handle large regions of separated flow where the turbulence is anisotropic. However the RSM model takes 50-60% more time when compared with a standard k-ε model. The LES model requires the most computational effort. However with the proper mesh refinement it is able to capture and predict anisotropic turbulence fields containing large vortical structures which are found in the wake of a bluff body. LES model will easily double the computational effort in comparison to k-ε model if the proper mesh refinement is utilized.

In the present study, the two-equation k-ε turbulence model is used. For this model, the Boussinesq approximation is assumed valid; it assumes that the turbulent stresses are proportional to the mean velocity gradients. Thus, specific Reynolds-stresses tensor and the turbulence kinetic energy can be calculated by the following equations [17]:

$$\tau_{ij} = 2\upsilon_t S_{ij} - \frac{2}{3} k \delta_{ij} \tag{4}$$

$$\frac{\partial k}{\partial t} + U_j \frac{\partial k}{\partial x_j} = \tau_{ij} \frac{\partial U_i}{\partial x_j} - \varepsilon + \frac{\partial}{\partial x_j} \left[(\upsilon + \upsilon_t / \sigma_k) \frac{\partial k}{\partial x_j} \right] \tag{5}$$

where ν_t is the kinematic turbulent viscosity (μ_t/ρ), S_{ij} is the mean strain-rate tensor, δ_{ij} Kronecker delta, σ_k is the turbulent Prandtl number, and k is the turbulent kinetic energy. The standard k-ε model is a semi-empirical turbulent model based on model transport equation for the turbulent kinetic energy k and its dissipation rate ε [18]. The model transport equation for k is derived from the exact equation, while the model transport equation for ε is obtained using physical reasoning and bears little resemblance to its mathematically exact counterpart [17]. The turbulence kinetic energy is calculated from equation 5 and the dissipation rate is calculated from

$$\frac{\partial \varepsilon}{\partial t} + U_j \frac{\partial \varepsilon}{\partial x_j} = C_{\varepsilon 1} \frac{\varepsilon}{k} \tau_{ij} \frac{\partial U_i}{\partial x_j} - C_{\varepsilon 2} \frac{\varepsilon^2}{k} + \frac{\partial}{\partial x_j} \left[(\upsilon + \upsilon_t / \sigma_e) \frac{\partial k}{\partial x_j} \right] \tag{6}$$

where $C_{\varepsilon 1}$, $C_{\varepsilon 2}$ are constants and σ_ε is the turbulent Prandtl numbers.

By combining k and ε, the turbulent viscosity is calculated as

$$\nu_t = C_\mu k^2 / \varepsilon \tag{7}$$

where Cμ is a constant. The model constants have the following values [18]: $C_{\varepsilon 1}$= 1.44, $C_{\varepsilon 2}$=1.92, σ_ε= 1.3, σ_k= 1.0, and Cμ= 0.09. These default values have been determined from experiments. They have been found to work fairly well for a wide range of turbulent flows.

BOUNDARY CONDITIONS AND CONVERGENCE

Six different free steam velocities (U) have been used varying between 12 m/s and 39 m/s. No-slip conditions are used along the walls. Uniform conditions are used for the freestream inlet. Initial conditions are obtained by specifying freestream conditions throughout the flowfield.

The converged solution is assumed to be achieved after satisfying the following conditions: (1) The residuals of the flow properties are less than 10^{-6}. (2) No changes in the centerline pressure profile are seen with the iterations (3) Global mass balance at the inlets and the outlets is satisfied.

$$\sum \dot{m}_{in} = \sum \dot{m}_{out}$$

and (4) Conservation of mass flow rates inside the computational domain is satisfied.

RESULTS AND DISCUSSION

In the present study, a total of six cases were computed. These cases were corresponding to free stream velocity of 43, 60, 82, 100, 120, and 140 km/hr. This is equivalent to a velocity range of 12 m/s-39 m/s.

Figure 2 shows the profile of the straemwise velocity for two different values of the free stream velocity, 12 m/s and 29 m/s at top of the van along the center plane at 1.25 m from the front of the van. The steamwise velocity is normalized with respect to the free stream velocity. The figure shows that the normalized velocity profiles are similar and the free stream velocity has no effect.

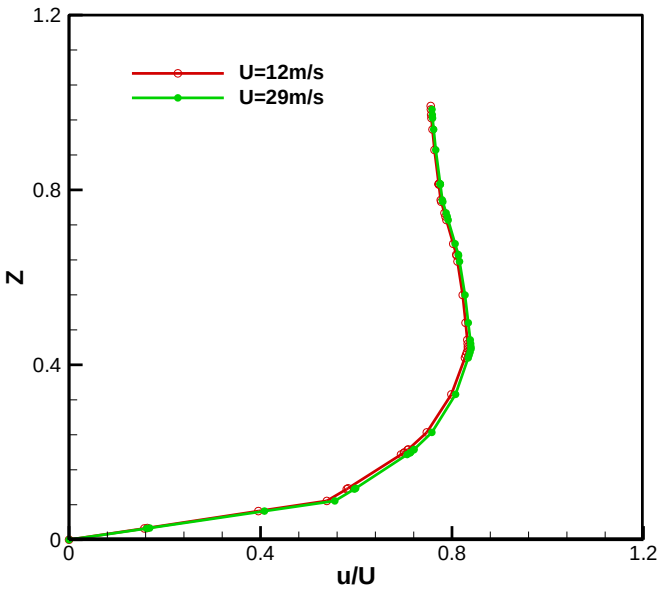

Figure 2 Normalized streamwise velocity profiles at the top of the van (x=1.25 m from the front)

Figure 3 shows the simulated streamlines in the center plane (y=0) for the six cases. Automobiles typically have large regions of separation flow at the rear of the body. This type of flow separation is typically referred to as bluff body separation and is the major contributor to the aerodynamic drag on the vehicle. To numerically predict this type of highly three-dimensional turbulent flowfield is very difficult and has eluded accurate predictions for researchers for many years. The figure

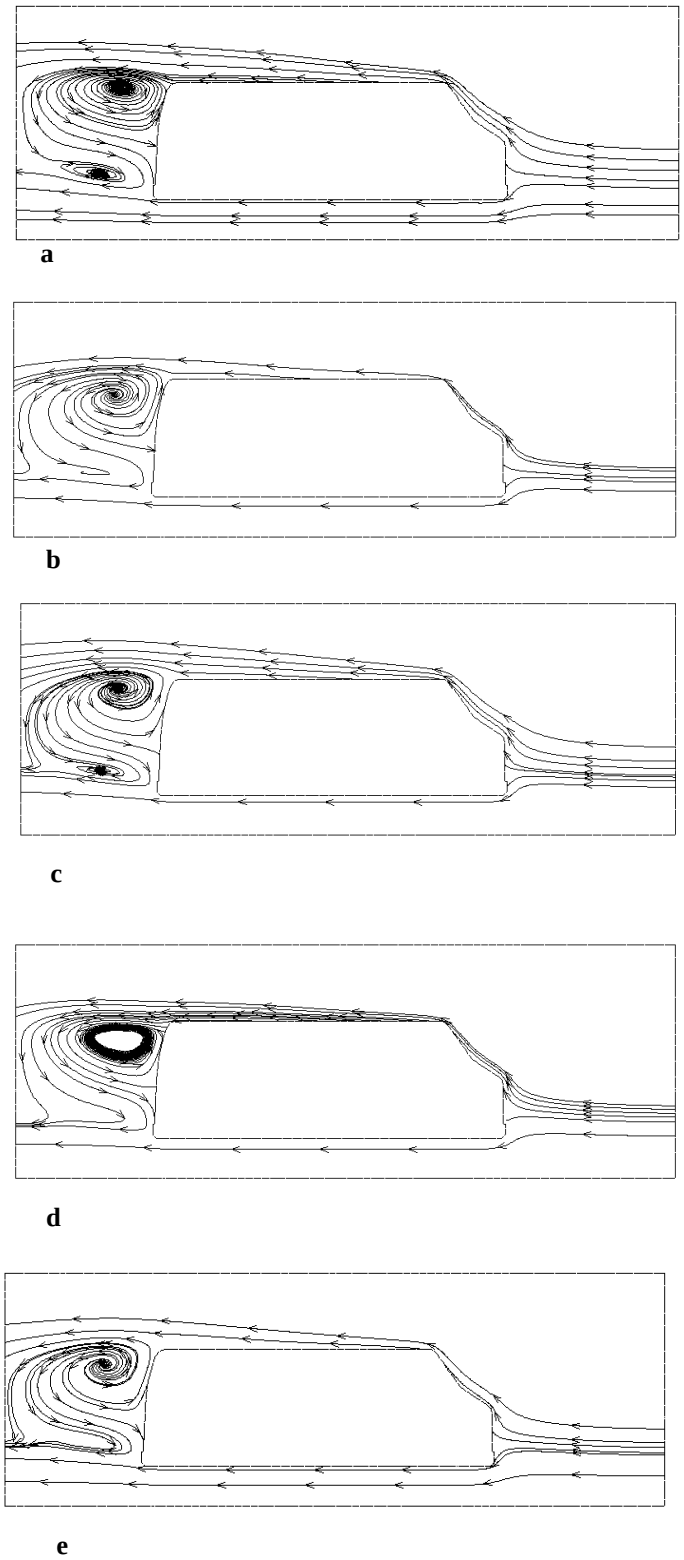

Figure 3 Center plane plot of velocity vectors (a)U=12 m/s, (b)U=23 m/s, (c) U=29 m/s, (d)U=33 m/s, and (e)U=39 m/s.

shows clearly the formation and the location of the separation region behind the van. It is well known that this region has a three-dimensional character. Also, it is seen that the flow accelerates around the leading edge of the top of the van. It is noticed that the flow behind the van is characterized by the recirculation vortex in the separation region. The vortex is located in the upper part of the van close to the top surface of the van and it is not highly affected by the change of the free stream velocity.

The profiles of the normalized stream wise velocity at the top of the van at different axial locations are shown in Figure 4. The profiles are presented for a free stream velocity of 33 m/s (120 km/hr) at distances of x=0.75 m, 1.5, 2.0 m, 2.5m and 3.0 m from the front of the van. It is shown that the velocity profile changed with the increase of the distance from the front of the van increase.

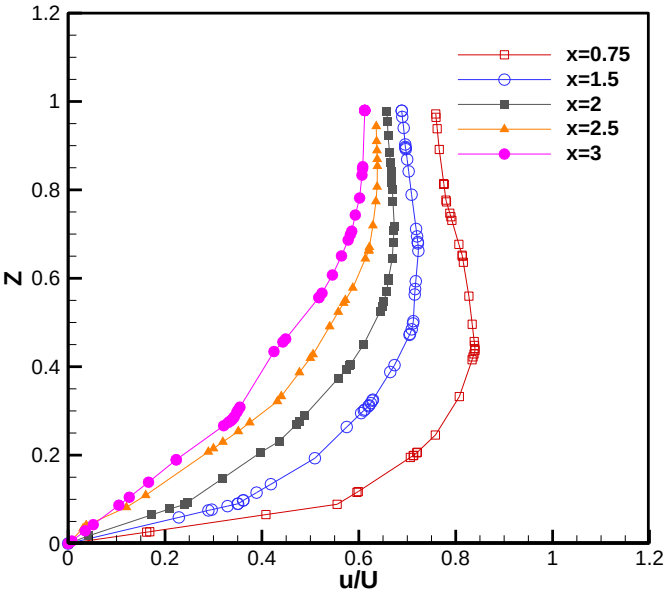

Figure 4 Normalized velocity profiles at the top of the van at different axial locations (U=33 m/s)

Figure 5 shows the normalized streamwise velocity profile in the center plane at different positions behind the van. The profiles are similar and the reversed flow region can be seen clearly. The reserved region is decreasing with the increase of the distance from the back of the van. The differences in the profiles can be attributed to their relative locations with respect to the centerline pressure gradient. The boundary layer is still recovering at x=0.75m from the flow acceleration at the leading edge and start to respond to the high pressures at the x=3.0.

The distribution of the pressure coefficient is presented in figures 6 and 7.

Figure 6 shows the profile at the top of the van in the center plane. The figure shows the pressure loss and recovery at the top of the van. It can be seen in figure 7 that the pressure coefficient has a minimum value near the lower part of the back of the van. The pressure coefficient increases again near the top of the van [2].

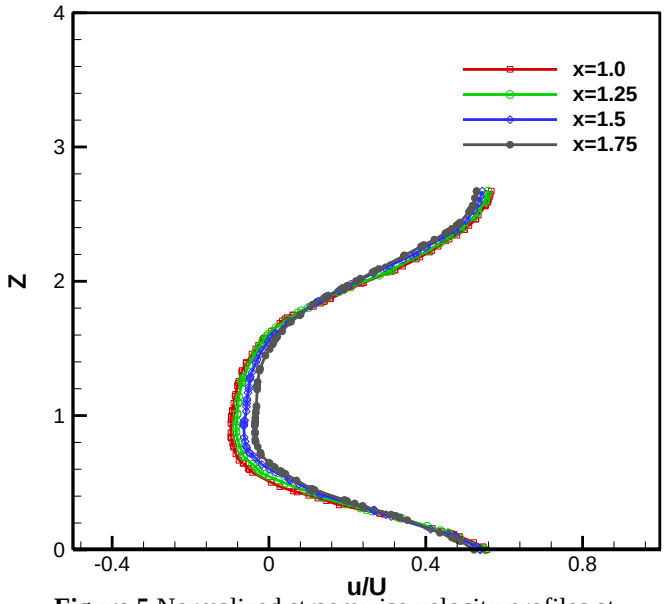

Figure 5 Normalized straemwise velocity profiles at different positions behind the van (U= 39m/s).

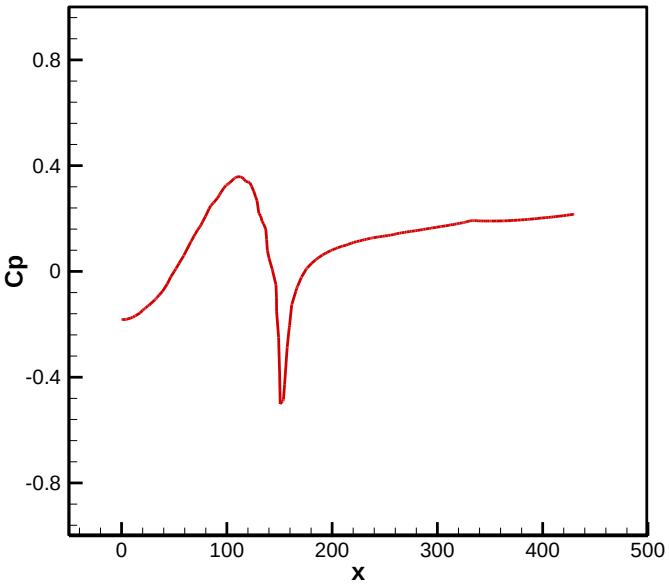

Figure 6 Distribution of pressure coefficient at the plan of symmetry (top of the van, U=23 m/s).

CONCLUSION

A numerical study is conducted to simulate the flow field around a model of a ford cargo van. Flowfield is obtained for different upstream velocities ranging from 12m/s to 39 m/s. Numerical analysis was carried out using a finite volume CFD code and using an unstructured grids. The separation region behind the van was captured. The upstream velocity has slight effect in the location of the separation region. Velocity profiles are found to be similar for different upsteam velocity values.

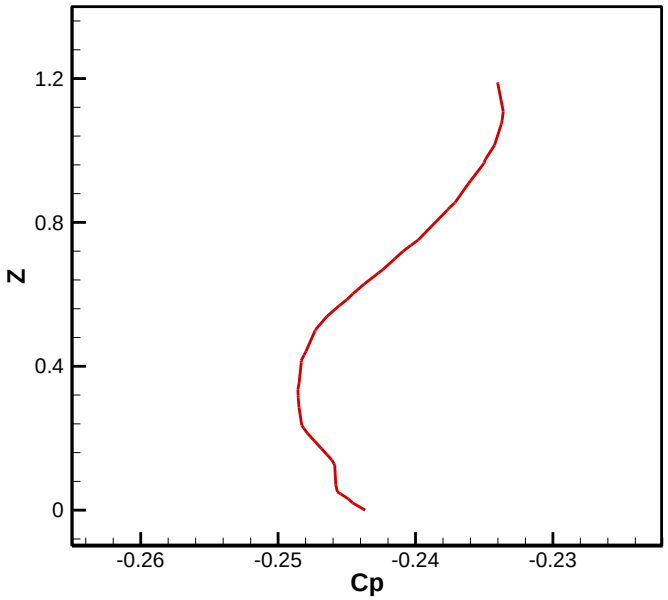

Figure 7 Distribution of pressure coefficient behind the van's trailing edge in the vertical direction (U=23 m/s)

REFERENCES

[1] Regert, T and Lajos, T., Numerical simulation of flow field in wheelhouse of cars, *Journal of Computational and Applied Mechanics*, Vol. 5, Num. 2, (2004), pp. 1-8.

[2] Khalighi, B., Jindal, S., Iaccarino, G., Aerodynamic flow around a sport utility vehicle—computational and experimental investigation, *Journal of Wind Engineering and Industrial Aerodynamics*, Volumes 107–108, August–September 2012, Pages 140–148.

[3] Gaylard, A.P., 2009. The appropriate use of CFD in the automotive design process. SAE Paper no. 2009-01-1162.

[4] Holloway, S., Leylek, J.H., York, W.D., Khalighi, B., Aerodynamics of a pickup truck: combined CFD and experimental study. *SAE International Journal of Commercial Vehicles*, Vol. 2, 2009, pp.88–100.

[5] Kitoh, K., Oshima, N., Yamamoto, H., Sebben, S., A CFD approach via large eddy simulation to the flow field with complex geometrical configurations: a study case of vehicle underbody flows. SAE Paper no. 2009-0-0332.

[6] Bagal, V., Mulemane, A., Aerodynamic drag simulation and validation of a crossover. SAE Paper no. 2010-01-0757.

[7] Keating, A., Shock, R., Chen, H., Lattice Boltzmann simulations of unsteady flow behind the Ahmed body. SAE Paper no. 2008-01-0740.

[8] Ahmed, S., Computational fluid dynamics. In: Hucho, W.H. (Ed.), Aerody- namics of Road Vehicles, 4th ed, 2009.

[9] Malviya, V., Mishra, R., Fieldhouse, J., CFD investigation of a novel fuel- saving device for articulated tractor-trailer combinations. *Engineering Appli- cations of Computational Fluid Mechanics*, Vol. 3, 2009, pp.587–607.

[10] Leinhart, H., & Becker, S., LDA Measurements of the Flow and Turbulence Structures in the Wake of a SImplified Car Model. Erlangen, Germany: University Erlangen.

[11] Krajnovic, S., & Davidson, L., Large-Eddy Simulation of the Flow Around Simplified Car Model. 2004 *SAE World Congress*.

[12] Ahmed, S.R and Ramm, G., "Some Salient Features of the Time-Averaged Ground Vehicle Wake", SAE 1984.

[13] Viswanath, P.R, "Drag reduction of Afterbodies by Controlled Separated Flows", *AIAA Journal*, Vol.39, Jan 2001.

[14] Kotha, S., "Three Dimensional Bluff Body Aerodynamic Analysis for Automotive and Automotive Racing Applications", Masters thesis, University of North Carolina, Charlotte, May 2005.

[15] Micklow, G., Kotha, S., and Abdel-Salam, T., three dimensional bluff body aerodynamic analysis for automotive and automotive racing applications, *proceedings of the SAE Motorsoprts Engineering Conference*, Dearborn, Michigan, December 2006.

[16] Fluent 14 User's Guide , Fluent Inc., New Hampshire, 2013.

[17] Wilcox, D. C., Turbulence Modeling for CFD, DCW Industries Incorporation, 1998.

[18] Launder, B. E., and Spalding, D. B, Lectures in Mathematical Models of Turbulence, Academic Press, London, England, 1972.